9. Wu, H. *et al.* T-cell accumulation and regulated on activation, normal T cell expressed and secreted upregulation in adipose tissue in obesity. *Circulation* **115**, 1029–1038 (2007).
10. Rausch, M.E., Weisberg, S., Vardhana, P. & Tortoriello, D.V. Obesity in C57BL/6J mice is characterized by adipose tissue hypoxia and cytotoxic T-cell infiltration. *Int. J. Obes. (Lond.)* **32**, 451–463 (2008).
11. Monney, L. *et al.* T_H1-specific cell surface protein Tim-3 regulates macrophage activation and severity of an autoimmune disease. *Nature* **415**, 536–541 (2002).
12. Brake, D.K., Smith, E.O., Mersmann, H., Smith, C.W. & Robker, R.L. ICAM-1 expression in adipose tissue: effects of diet-induced obesity in mice. *Am. J. Physiol. Cell Physiol.* **291**, C1232–C1239 (2006).
13. Traktuev, D.O. *et al.* A population of multipotent CD34-positive adipose stromal cells share pericyte and mesenchymal surface markers, reside in a periendothelial location and stabilize endothelial networks. *Circ. Res.* **102**, 77–85 (2008).
14. Nishimura, S. *et al.* Adipogenesis in obesity requires close interplay between differentiating adipocytes, stromal cells and blood vessels. *Diabetes* **56**, 1517–1526 (2007).
15. Cinti, S. *et al.* Adipocyte death defines macrophage localization and function in adipose tissue of obese mice and humans. *J. Lipid Res.* **46**, 2347–2355 (2005).
16. Sallusto, F., Lenig, D., Forster, R., Lipp, M. & Lanzavecchia, A. Two subsets of memory T lymphocytes with distinct homing potentials and effector functions. *Nature* **401**, 708–712 (1999).
17. Lumeng, C.N., Bodzin, J.L. & Saltiel, A.R. Obesity induces a phenotypic switch in adipose tissue macrophage polarization. *J. Clin. Invest.* **117**, 175–184 (2007).
18. Kintscher, U. *et al.* T-lymphocyte infiltration in visceral adipose tissue: a primary event in adipose tissue inflammation and the development of obesity-mediated insulin resistance. *Arterioscler. Thromb. Vasc. Biol.* **28**, 1304–1310 (2008).
19. Miller, R., Wen, X., Dunford, B., Wang, X. & Suzuki, Y. Cytokine production of $CD8^+$ immune T cells but not of $CD4^+$ T cells from *Toxoplasma gondii*–infected mice is polarized to a type 1 response following stimulation with tachyzoite-infected macrophages. *J. Interferon Cytokine Res.* **26**, 787–792 (2006).
20. Sakaguchi, S. *et al.* $Foxp3^+$ $CD25^+$ $CD4^+$ natural regulatory T cells in dominant self-tolerance and autoimmune disease. *Immunol. Rev.* **212**, 8–27 (2006).
21. Taams, L.S. *et al.* Modulation of monocyte/macrophage function by human $CD4^+CD25^+$ regulatory T cells. *Hum. Immunol.* **66**, 222–230 (2005).
22. Mahajan, D. *et al.* $CD4^+CD25^+$ regulatory T cells protect against injury in an innate murine model of chronic kidney disease. *J. Am. Soc. Nephrol.* **17**, 2731–2741 (2006).

ONLINE METHODS

Mice. We obtained Male C57BL/6J, *ob/ob* and *Cd8a*-deficient mice from Charles River Japan or Jackson Laboratories. All mice were housed under a 12-h light-dark cycle and allowed free access to food. To examine the time-course of changes in stromal vascular cell populations in adipose tissue under conditions of diet-induced obesity, we divided C57BL/6 mice into two groups and fed either a standard chow diet (6% fat, Oriental Yeast Company) or a high-fat diet (D12492, 60 Kcal% fat, Research Diets) from the age of 4 weeks.

To examine the effects of CD8 depletion on the initiation and development of adipose inflammation, we started antibody administration before the establishment of DIO. We fed male C57BL/6 mice a high-fat diet for 8 weeks, beginning when they were 4-weeks-old, and we intraperitoneally administered either CD8-specific antibody (3 μg per g body weight, 1 mg ml^{-1} solution, Biolegend) or control rat IgG (Sigma, 1 mg ml^{-1} PBS solution) weekly over the same period. We examined the mice at 12 weeks old (**Fig. 2** and **Supplementary Fig. 7**). We validated depletion of $CD8^+$ T cells by antibody as shown in **Supplementary Figure 11**.

To assess the effects of CD8 depletion on preestablished adipose inflammation in DIO mice, we fed C57BL/6 mice a high-fat diet, beginning when they were 9-weeks-old. Ten weeks later, we randomly assigned the 19-week-old obese mice to two groups and we intraperitoneally administered either CD8-specific antibody (120 μg per mouse) or control IgG three times per week for 2 weeks (total of six administrations). Age-matched lean C57BL/6 mice fed a normal chow diet served as controls. At 21 weeks, we performed oral glucose and insulin tolerance tests and then killed the mice for analysis of their adipose tissue (**Fig. 3** and **Supplementary Fig. 9**).

To assess the effects of CD8-deficient and adoptive transfer of $CD8^+$ T cells on adipose inflammation, we fed *CD8a*$^{-/-}$ mice either normal chow or a high-fat diet for 8 weeks, beginning when they were 6-weeks-old. We intravenously administered either 5×10^6 splenic $CD8^+$ T cells or control PBS weekly over the same period. We examined the *CD8a*$^{-/-}$ mice at 14-weeks-old. We prepared $CD8^+$ splenic T cells from 7-week-old C57BL/6 mice (**Fig. 4** and **Supplementary Fig. 10**). All experiments were approved by the Institutional Committee for Animal Research of The University of Tokyo and strictly adhered to the guidelines for animal experiments of The University of Tokyo.

Isolation of the stromal vascular fraction and flow cytometry. We isolated stromal vascular cells using previously described methods with some modifications. We killed the mice after general anesthesia after systemic heparinization. We removed the epididymal and subcutaneous adipose tissues and then minced it into small pieces (~2 mm). We vigorously agitated the pieces in PBS supplemented with 1 μg ml^{-1} heparin for 30 s to remove any circulating blood cells and then centrifuged the suspension at 1,000*g* for 8 min. We collected floating pieces of adipose tissue and incubated them for 20 min in collagenase solution (2 mg ml^{-1} of collagenase type 2 (Worthington) in Tyrode buffer (containing 137 mM NaCl, 5.4 mM KCl, 1.8 mM $CaCl_2$, 0.5 mM $MgCl_2$, 0.33 mM NaH_2PO_4, 5 mM HEPES and 5 mM glucose)) with gentle stirring. We then centrifuged the digested tissue again at 1,000*g* for 8 min. We resuspended the resultant pellet containing the stromal vascular fraction into PBS and filtered it through a 70-μm mesh. We washed the cells twice with PBS, incubated for 10 min in erythrocyte-lysing buffer (Becton Dickinson) as previously described[3], and we finally resuspended them in PBS supplemented with 3% FBS. We incubated these isolated cells with either labeled monoclonal antibody or isotype control antibody (eBioscience and BD Pharmingen) and analyzed by flow cytometry with a Vantage flow cytometer (Becton Dickinson) and FlowJo (Tree Star, Inc.) software. We used propidium iodide (Invitrogen) to exclude dead cells. We validated flow cytometric identification of M1 ($F4/80^+CD11c^+$) and M2 ($F4/80^+CD11c^-$) macrophages with CD11c markers as described in the **Supplementary Methods** and **Supplementary Figure 12**.

Immunohistochemistry. We stained and visualized whole-mount adipose tissue as previously described[14].

CFSE proliferation assay of $CD8^+$ T cells. We isolated splenic $CD8^+$ T cells from 7-week-old C57BL/6 mice and incubated the isolated $CD3^+$ $CD8^+$ cells with 5 μM CFSE (CellTrace CFSE Cell Proliferation Kit, Invitrogen). After staining, we incubated 2×10^5 cells in DMEM supplemented with 3% FBS for 2 d, with or without 20 mg of minced epididymal white adipose tissue prepared from either 20-week-old lean mice fed a normal chow diet or DIO mice fed a high-fat diet for 16 weeks. We harvested the $CD8^+$ cells and then analyzed them by flow cytometry to examine the proliferation status.

Differentiation of peripheral blood monocytes into macrophages. We isolated peripheral blood monocytes ($CD11b^{high}Gr\text{-}1^-$) from lean 7-week-old C57BL/6 mice. In the lower wells of a 24-well Multiwell Boyden chamber (Becton Dickinson), we cultured 5×10^4 monocytes per well in DMEM supplemented with 3% FBS, with or without 10 mg of minced epididymal adipose tissue prepared from 7-week-old lean mice in the upper wells. Also in the upper wells, we cultured 5×10^4 $CD3^+CD8^+CD4^-$ T cells, which we isolated from epididymal adipose tissues of 20-week-old lean or DIO mice. We incubated the cells for 7 d, after which the cells in the upper wells were collected, stained for CD11b, F4/80 and CD68, and assayed by flow cytometry for the differentiated macrophage fractions ($CD11b^+F4/80^+CD68^+$).

Migration of RAW264.7 and peritoneal macrophages. We isolated $CD8^+$ T cells from blood collected from C57BL/B6J mice after cardiac puncture. We isolated and cultured $CD3^+CD8^+$ cells were in DMEM supplemented with 3% FBS. To activate $CD8^+$ T cells, we cultured the cells with recombinant IL-2 (20 U ml^{-1}; Sigma), Dynabeads CD3/CD28 T Cell Expander (a bead-to-cell ratio of 1:1) and 2-mercaptoethanol (50 μM). After 120 h of culture, we aspirated the culture medium and performed migration assay using Boyden chambers with 8-μm pore inserts (Becton Dickinson). We cultured RAW264.7 and peritoneal macrophages in the upper wells, and we added the conditioned medium to the lower wells. We used fresh DMEM supplemented with 5% FBS as a control. To inhibit MCP-1 activity, we added a neutralizing antibody (5 μg ml^{-1} antibody to MCP-1, clone 2H5, Biolegend) to the conditioned medium.

TNF-α production in macrophages cocultured with $CD8^+$ cells. We isolated $F4/80^+$ $CD11b^+$ macrophages from epididymal adipose tissue from lean 7-week-old C57Bl/B6J mice, and we isolated $CD3^+CD8^+CD4^-$ T cells from epididymal adipose tissue from 20-week-old lean or DIO mice. We then added the adipose macrophages to the upper wells of a Multiwell Boyden chamber (Becton Dickinson) (5×10^4 cells per well), and we added the same number of $CD8^+$ T cells to the lower wells, after which we cultured the cells in DMEM supplemented with 3% FBS for 7 d. We assessed intracellular production of TNF-α by flow cytometry using an intracellular cytokine production detection kit (Cytofix/Cytoperm Fixation/Permeabilization Solution Kit, BD Pharmingen).

Human subjects. We acquired subcutaneous adipose tissue from healthy female donors undergoing liposuction of the abdomen or thighs (after obtaining their consent). We examined expression of *CD8a* in the tissue. We processed samples comprised of 1 g of each specimen by digestion with collagenase and then centrifuged to isolate the stromal vascular fractions. We purified total RNA using Trizol (Invitrogen) and determined relative mRNA levels using real-time PCR. This study was approved by the Ethics Committee of The University of Tokyo Hospital.

Statistical analyses. We expressed the results as means ± s.e.m. We determined the statistical significance of differences between two groups using Student's *t* tests, and we evaluated differences among three groups by analysis of variance followed by *post-hoc* Bonferroni tests. Values of $P < 0.05$ were considered significant.

doi:10.1038/nm.1964

STEM CELLS
THE STEM CELL NICHE

The Actin Polymerization Regulator WAVE2 Is Required for Early Bone Marrow Repopulation by Hematopoietic Stem Cells

TAKUNORI OGAERI, KOJI ETO, MAKOTO OTSU, HIDEO EMA, HIROMITSU NAKAUCHI

Division of Stem Cell Therapy, Center for Stem Cell and Regenerative Medicine, The Institute of Medical Science, University of Tokyo, Tokyo, Japan

Key Words. Hematopoietic stem cells • Engraftment • Knockdown • Actin polymerization • Rac

ABSTRACT

The Rho GTPase family members play essential roles in hematopoiesis. Of these, Rac1 is thought to be required for the appropriate spatial localization of hematopoietic stem and/or progenitor cells (HSPCs) within the bone marrow (BM), whereas Rac2 likely plays a role in BM retention of HSPCs. To elucidate the molecular mechanisms underlying Rac-mediated functions in hematopoietic stem cells (HSCs), we studied Wiskott-Aldrich syndrome protein family verprolin-homologous proteins (WAVEs), the specific effectors downstream of the Rac GTPases in actin polymerization. We here showed that $CD34^{-/low}c\text{-}Kit^{+}Sca\text{-}1^{+}lineage^{-}$ HSCs ($CD34^{-}KSL$ HSCs) express WAVE2 but neither WAVE1 nor WAVE3. Because WAVE2 knockout mice are embryonic-lethal, we utilized HSCs in which the expression of WAVE2 was reduced by small interfering RNA. We found that knockdown (KD) of WAVE2 in HSCs affected neither in vitro colony formation nor cell proliferation but did impair in vivo long-term reconstitution. Interestingly, WAVE2 KD HSCs exhibited unaltered homing but showed poor BM repopulation detected as early as day 5 after transplantation. The mechanistic studies on WAVE2 KD HSCs revealed modest but significant impairment in both cobblestone-like area-forming on stromal layers and actin polymerization upon integrin ligation by fibronectin. These results suggested that WAVE2-mediated actin polymerization, potentially downstream of Rac1, plays an important role in intramarrow mobilization and proliferation of HSCs, which are believed to be crucial steps for long-term marrow reconstitution after transplantation. STEM CELLS *2009;27:1120–1129*

Disclosure of potential conflicts of interest is found at the end of this article.

INTRODUCTION

Adult hematopoietic stem cells (HSCs) exhibit self-renewal and undergo multilineage differentiation presumably within a specific bone marrow (BM) microenvironment, referred to as the BM niche [1–4]. Both extrinsic and intrinsic factors are required for the maintenance of HSC functions [3, 4]. HSC status is believed to be controlled within the BM niche by orchestrated signaling circuits mediated by a variety of molecules including stem cell factor (SCF)/c-Kit, thrombopoietin (TPO)/c-Mpl, angiopoietin-1/Tie2, Wnt, Notch, bone morphogenic proteins, Ca^{2+}, and chemokine (C-X-C motif) ligand 12 (or stromal-derived factor-1)/CXC receptor 4 (CXCR4) [2–6]. Also well documented is that cell-to-cell or cell-to-extracellular matrix interaction itself is crucial for the execution of HSC functions in the niche system [7]. In the setting of transplantation, HSCs must take several steps to achieve successful long-term engraftment, which include transendothelial migration into the BM cavity from circulation (homing), settling in the BM niche (lodging and retention), and intraniche proliferation and multilineage differentiation (repopulation). The interactions between HSCs and various extracellular elements affect these multistep processes [8].

Rho GTPases are molecules known to integrate intracellular signals downstream of CXCR4, c-Kit, and integrins [5, 6, 9]. Rho, Rac, and Cdc42 belong to the Rho GTPase family. Rac and Cdc42 are primarily required for actin polymerization leading to cell adhesion, spreading, migration, and pattern formation [10, 11]. Actin cytoskeletal structures such as filopodia and lamellipodia are formed by actin polymerization [12]. Actin polymerization requires the actin-related protein two-third (Arp2/3) complex, which is activated by Cdc42 signaling via Wiskott-Aldrich syndrome protein (WASp) and N-WASp or by Rac signaling via members of the WASp family verprolin-homologous protein (WAVE) [11, 13].

Both Rac1 and Rac2 are expressed in hematopoietic lineages, but they exhibit distinct functions in hematopoietic stem and/or progenitor cells (HSPCs) [14]. $Rac1^{-/-}$HSPCs show defective hematopoietic repopulation after transplantation. This has been mainly ascribed to early engraftment failure, not to defective long-term repopulation potential [14–16]. Impaired microlocalization has been suggested to cause this engraftment failure. In contrast, $Rac2^{-/-}$HSPCs showed normal early

Author contributions: T.O.: performance of study, collection of data, final approval of manuscript; K.E. and M.O.: conception and design of study, manuscript writing, data analysis and interpretation, final approval of manuscript; H.E.: design of study, data interpretation, final approval of manuscript; H.N.: financial support, administrative support, final approval of manuscript.

Correspondence: Hiromitsu Nakauchi, M.D., Ph.D., Division of Stem Cell Therapy, Center for Stem Cell and Regenerative Medicine, Institute of Medical Science, University of Tokyo, 4-6-1 Shirokanedai, Minato-ku, Tokyo 108-8639, Japan. Telephone: 81-3-5449-5330; Fax: 81-3-5449-5451; e-mail: nakauchi@ims.u-tokyo.ac.jp Received July 14, 2008; accepted for publication February 12, 2009; first published online in STEM CELLS *EXPRESS* February 20, 2009. 1066-5099/2009/$30.00/0 doi: 10.1002/stem.42

engraftment but were at a disadvantage in competitive repopulation, presumably caused by defective adhesion to and impaired retention within the BM niche [14–16]. Although these studies have paved a way to understand the molecular regulation of HSPC homing, engraftment, and mobilization, little is known which effectors lie downstream of Rac and how they function in HSCs. We therefore performed the current study to examine the roles of WAVEs in HSC functions.

We showed that $CD34^{-/low}$c-Kit^{+}Sca-1^{+}lineage^{-} HSCs ($CD34^{-}$KSL HSCs) express only WAVE2 among the WAVE family, and that knockdown (KD) of WAVE2 reduces the levels of long-term repopulation, possibly resulting from poor early BM repopulation by HSCs. As detailed analyses revealed many similarities of phenotypes between HSCs deficient in Rac1 and WAVE2 KD HSCs, we concluded that WAVE2 likely acts as the key effector of Rac1 in HSCs during early repopulation of BM after transplantation.

Materials and Methods

Mice

All animal and recombinant DNA experiments were performed with approval of the Institutional Animal Care and Use Committee of the Institute of Medical Science, University of Tokyo. C57BL/6 (B6)-Ly5.1 mice were from Sankyo Laboratory (Tsukuba, Japan, http://www.sankyolabo.co.jp) and B6-Ly5.2 mice were from Japan SLC (Shizuoka, Japan, http://jslc.co.jp).

Purification of $CD34^{-}$KSL HSCs and $CD34^{+}$KSL Cells

$CD34^{-}$KSL HSCs and $CD34^{+}$KSL progenitor cells were purified from B6 mouse BM as described [17]. Multicolor flow cytometry analysis and cell sorting were performed using a fluorescence-activated cell sorting (FACS) Vantage SE (Becton, Dickinson and Company, San Diego, CA, http://www.bd.com) or a MoFlo Cell Sorter (Beckman Coulter, Fullerton, CA, http://www.beckmancoulter.com). Anti-mouse antibodies conjugated with biotin, fluorescein isothiocyanate, phycoerythrin (PE), allophycocyanin (APC), or PE-cyanin 7 (PE-Cy7) were from BD Biosciences (San Diego, CA, http://www.bdbiosciences.com) or Invitrogen (San Diego, CA, http://www.invitrogen.com). Streptavidin-alexa 594-conjugated rat IgG secondary antibody was from Molecular Probes Inc. (Tokyo, Japan, http://probes.invitrogen.com) or Invitrogen Japan (Tokyo, Japan). Purity of sorted cell fractions was consistently >98%.

Gene-KD Vector Preparation

The FG12 lentiviral vector used in KD procedures was a generous gift from Drs. X. Qin and D. Baltimore (California Institute of Technology, Pasadena, CA) [18]. The FG12 vector construct contains a 5′ long terminal repeat (LTR), multiple cloning sites, and a ubiquitin C promoter-driven enhanced green fluorescent protein, followed by a 3′ LTR. We followed published protocols for the use of WAVE2 short hairpin type small interfering RNAs (shRNAs) [19, 20]. The FG12 lentivector with scramble control shRNA was used as a control vector. We used control shRNA sequences known to not affect WAVE2 expression [20]. Concentrated viral supernatant samples were produced by calcium phosphate transfection of 293T cells and viral titers were determined as described [20].

Gene Transduction of Mouse $CD34^{-}$KSL HSCs

HSCs from B6-Ly5.2 wild-type or $WAVE2^{\pm}$ mice [19] (8–11 weeks old) were sorted at 50 cells per well into 96-well plates that were precoated with Retronectin (10 μg/ml; Takara Bio, Shiga, Japan, http://www.takara.co.jp) and contained α-minimal essential medium (α-MEM) supplemented with 1% fetal bovine serum (FBS), 100 ng/ml mouse SCF (Peprotech, Tokyo, Japan, http://www.peprotech.com), and 100 ng/ml human TPO (Peprotech). Following 24 hours of preincubation, recombinant lentiviral supernatant was added to wells at a multiplicity of infection of 600 or 1,200 and the plates were incubated for the following 14 hours in the presence of SCF, TPO, and protamine sulfate (10 μg/ml) (Fig. 2A). To maximize the effect of shRNA, the cells were further incubated for another 4 days with medium shifted from α-MEM 1% FBS to S-Clone SF-O3 (S-Clone, Sanko Junyaku, Tokyo, http://www.sanko-junyako.co.jp) supplemented with 1% bovine serum albumin (BSA), 50 ng/ml SCF, and 50 ng/ml TPO. Transduction efficiency was consistently over 90% as determined by green fluorescent protein (GFP) expression.

Semiquantitative Reverse Transcriptase-Polymerase Chain Reaction

Total RNA was extracted from cell samples using TRIzol reagent (Invitrogen). First strand cDNA was synthesized from RNA samples with Superscript II Reverse Transcriptase (Invitrogen). cDNA copy numbers were normalized against glyceraldehyde-3-phosphate dehydrogenase (*GAPDH*) copy numbers calculated based on quantitative polymerase chain reaction (PCR) results using the TaqMan rodent GAPDH control reagent (Perkin-Elmer Applied Biosystems, Foster City, CA, http://www.appliedbiosystems.com) [21]. The normalized cDNA was amplified with each primer pair for 38 cycles of three-step PCR consisting of 95°C for 15 seconds, 60°C for 15 seconds, and 72°C for 20 seconds.

Primer sets used were as follows: *WAVE1*, forward primer (5′-GAAAGTGCCAAGAGCACCTC-3′) and reverse primer (5′-AGCTGGGTGAAGAACACCAG -3′); *WAVE2*, forward primer (5′-TCCGAGTGCTTCCTTCAACT-3′) and reverse primer (5′-CCCAGGAAACACAGGTGACT-3′); *WAVE3*, forward primer (5′-ATCCTCCGAGGGATCTCTGT-3′) and reverse primer (5′-GGTGAGGAGGAGTGGGGTAT-3′); *GAPDH*, forward primer (5′-CTTCACCACCATGGAGAAGGC-3′) and reverse primer (5′-GGCATGGACTGTGGTCATGAG-3′).

Immunocytostaining for WAVE1, WAVE2, or WAVE3

Cells were immunostained as described previously [22, 23]. Cells were directly sorted by flow cytometry into a droplet of serum-free culture medium on a poly-L-lysine-coated glass slide and incubated for 30 minutes at 37°C or 4°C. After fixation with 2% paraformaldehyde, cells were incubated for 12-hour at 4°C with rabbit polyclonal anti-WAVE1, -WAVE2, or -WAVE3 antibodies [19, 20] at a dilution of 1:200. After washes, cells were incubated for 30 minutes at room temperature with Alexa Fluor 647-labeled goat anti-rabbit IgG secondary antibody (Molecular Probes/Invitrogen Japan) at a dilution of 1:500 and nuclei were marked by 4,6-diamino-2-phenylindole staining. A Leica TCS SP2 AOBS confocal microscope (Leica Microscopy System, Wetzlar, Germany, http://www.leica-microsystems.com) was used to visualize fluorescent signals.

In Vitro Colony Assays and Cell Proliferation Assays

In vitro colony assays to evaluate colony-forming units (CFUs) were performed with methylcellulose medium (Stem Cell Technologies, Vancouver, BC, Canada, http://www.stemcell.com) containing 30% FBS, 10 ng/ml mouse SCF, 10 ng/ml human TPO, 10 ng/ml mouse interleukin (IL)-3

(Peprotech), and 2 units/ml human erythropoietin (EPO; Peprotech) in 35-mm dishes. Cells were incubated for 14 days at 37°C in a humidified atmosphere with 5% CO_2. Colonies were enumerated under an inverted microscope and classified based on cell composition in each colony by morphological analysis of cytospin cells after May–Grünwald–Giemsa staining. Cell proliferation was assessed in liquid culture using 96-well culture plates. GFP^+ HSCs ($n = 100$) were directly sorted into each well; the wells contained S-Clone supplemented with 1% BSA, SCF, TPO, IL-3, and EPO. Cell numbers were determined at indicated time points using Flow-Count beads (Beckman Coulter) and a FACS Calibur flow cytometer (Becton, Dickinson and Company).

Competitive Repopulation Assays

Competitive repopulation assays were performed using the Ly5 congenic mouse system (Fig. 2A). Recipient mice (B6-Ly5.1) were lethally irradiated at a dose of 9.5 Gy. Transduced cells (equivalent to 50 $CD34^-KSL$ cells input) from B6-Ly5.2 mice were mixed with 2×10^5 competitor BM cells from B6-Ly5.1 mice and infused by vein into recipients. Peripheral blood cells were taken 16 weeks post-transplantation and were analyzed by flow cytometry for reconstitution levels in myeloid (APC-conjugated $Mac\text{-}1^+/Gr\text{-}1^+$), B-lymphoid (PE-Cy7-conjugated $B220^+$), and T-lymphoid (PE-conjugated $CD4^+/CD8^+$) lineages, together with Ly5 markers.

Early Repopulation Assays

To evaluate early BM repopulation by HSCs, we measured the numbers of CFUs in recipient BM on days 3, 5, and 7 post-transplantation. The transduced HSCs (equivalent to 50 input cells) were transplanted without competitor cells into B6-Ly5.1 mice lethally irradiated at a dose of 9.5 Gy. At days 3, 5, and 7 post-transplantation, BM cells were obtained from both femora of each recipient mouse and subjected to in vitro colony-forming assays. GFP^+ colonies were enumerated at day 12 of culture. Colonies formed by BM cells were exclusively of $Ly5.2^+$ cell origin (donor HSC) as verified in representative experiments (data not shown).

Cobblestone-Like Area-Forming Assays

For cobblestone-like area-forming cell (CAFC) assays, infected HSCs ($n = 50$) in a 200-μL well of a 96-well plate were dispersed and maintained in the presence of 1% BSA, 50 ng/ml SCF, and 50 ng/ml TPO. At day 4 of culture, 1/10th of that volume (20 μl), inferred to contain 1/10th of the infected HSCs, was added to each well of a 6-well plate containing C3H10T1/2 cells irradiated at a dose of 50 Gy (RIKEN Biosource, Tsukuba, Japan, http://www.brc.riken.go.jp/inf/en/index.shtml). After coculture for 10 days (culture volume, 2 ml; Dulbecco's modified Eagle's medium supplemented with 10% FBS, 10 ng/ml SCF, and 10 ng/ml TPO), GFP^+ CAFCs per well were counted by using epifluorescent microscope DM IRBE equipped with a recording system (Leica Microscopy System). Experiments were performed twice independently.

Statistical Analysis

Data were expressed as means ± SD and subjected to Student's unpaired t test or one-way ANOVA test by using Prism 4 software (GraphPad, San Diego, CA, http://www.graphpad.com). A level of $p < .05$ was considered significant.

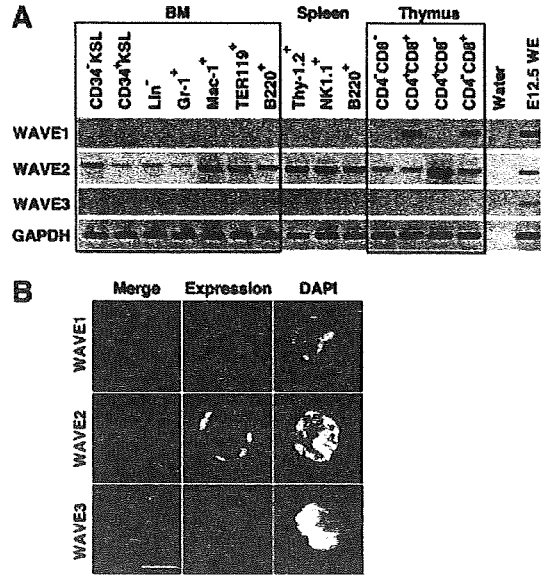

Figure 1. $CD34^-KSL$ hematopoietic stem cells (HSCs) express WAVE2 but not WAVE1 or WAVE3. **(A):** Expression of *WAVE1*, *WAVE2*, *WAVE3*, and *GAPDH* at RNA level was examined by semiquantitative reverse transcription-polymerase chain reaction analysis. cDNAs were prepared, in BM, from $CD34^-KSL$ cells, $CD34^+KSL$ cells, lineage marker$^-$ cells, $Gr\text{-}1^+Mac\text{-}1^+$ neutrophils/macrophages, $TER119^+$ erythroblasts, and $B220^+$ B-lymphoid cells; in spleen, from $B220^+$ B-lymphoid cells, $Thy\text{-}1.2^+$ T-lymphoid cells, and $Nk\text{-}1.1^+$ NK/NKT cells; and in thymus, from $CD4^-CD8^-$, $CD4^+CD8^+$, $CD4^+CD8^-$, and $CD4^-CD8^+$ T-lymphoid cells of adult B6 mice. E12.5 WE served as a positive control. **(B):** Protein expression of WAVE1, WAVE2, or WAVE3 was examined by immunofluorescent staining. The images of representative $CD34^-KSL$ HSCs stained with each anti-WAVE antibody followed by staining with Alexa fluor-647 (red)-rabbit anti-rat IgG antibody are shown. Nuclei were marked by DAPI staining (blue). Scale bar = 10 μm. Abbreviations: BM, bone marrow; DAPI, 4,6-diamino-2-phenylindole; E12.5 WE, embryonic day 12.5 whole embryos; GAPDH, glyceraldehyde-3-phosphate dehydrogenase; KSL, $c\text{-}Kit^+Sca\text{-}1^+lineage^-$; WAVE, Wiskott-Aldrich syndrome protein family verprolin-homologous protein.

Results

WAVE Expression in HSCs

We first examined the expression of WAVE isoforms by semiquantitative reverse transcriptase (RT)-PCR analysis in various hematopoietic cell populations including $CD34^-KSL$ HSCs [17] and $CD34^+KSL$ progenitors [17] (Fig. 1A). *WAVE2* expression was detected in most populations at varying levels, whereas *WAVE1* and *WAVE3* expression was rarely detected in the tested samples. Of note was that the expression of *WAVE2*, but not of *WAVE1* or *WAVE3*, was detected in $CD34^-KSL$ HSCs. *WAVE2* expression levels were lower in $CD34^+KSL$ cells, suggesting specific functions of WAVE2 in HSCs (Fig. 1A). Expression of WAVE2 in single HSC at the protein level was confirmed by immunostaining (Fig. 1B). The absence of WAVE1- and WAVE3-fluorescent signals was consistent with the RT-PCR results. These results indicate that among WAVE family members, WAVE2 may play a principal role in a signaling pathway downstream of Rac in HSCs.

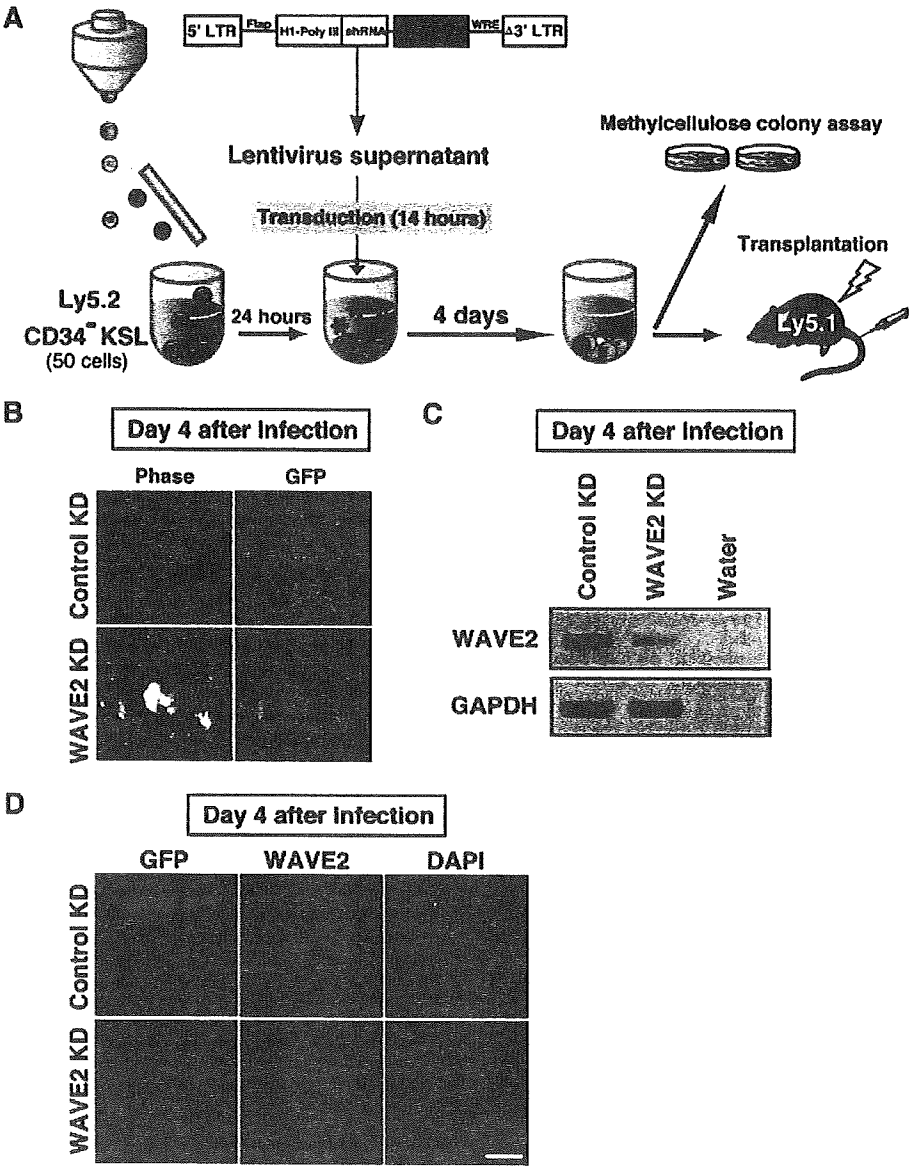

Figure 2. Lentivirus-mediated shRNA transduction of CD34⁻KSL hematopoietic stem cells (HSCs) leads to effective gene KD of WAVE2. **(A):** The experimental scheme is shown. CD34⁻KSL cells were sorted into U-bottom 96-well plates at 50 cells per well. Following preincubation of HSCs in the presence of thrombopoietin and stem cell factor for 24 hours, lentivirus infection was carried out in the presence of protamine sulfate for 14 hours. The cells were then cultured for another 4 days to allow sufficient KD action (expression of EGFP). Transduced cells were then subjected to either in vitro colony-forming unit assays or in vivo long-term repopulation assays. **(B):** The photomicrographs of transduced cells 4 days after infection are shown. Over 90% of cells expressed GFP after infection. **(C):** Expression of *WAVE2* and *GAPDH* mRNA was assessed by reverse transcription-polymerase chain reaction at day 4 after infection. The HSCs in which WAVE2 shRNA was transduced exhibited reduced *WAVE2* expression. **(D):** Immunostaining of WAVE2 in cells at day 4 after infection is shown. Scale bar= 10 μm. Abbreviations: DAPI, 4,6-diamino-2-phenylindole; GAPDH, glyceraldehyde-3-phosphate dehydrogenase; GFP, green fluorescent protein; KD, knockdown; KSL, c-Kit⁺Sca-1⁺lineage⁻; LTR, long terminal repeat; shRNA, short hairpin RNA; Ubi C-EGFP, ubiquitin C promoter-driven enhanced green fluorescent protein; WAVE, Wiskott-Aldrich syndrome protein family verprolin-homologous protein; WRE, woodchuck hepatitis virus posttranscriptional regulatory element.

KD of WAVE2 in HSCs

Mice deficient in WAVE2 die at embryonic days 11.5–12.5 because of defective vasculogenesis caused by the lack of lamellipodium formation by endothelial cells and smooth muscle cells [24]. We therefore utilized a lentiviral transduction gene KD strategy to reduce the expression of WAVE2 in HSCs. Shown in Figure 2A is the experimental scheme for transduction of shRNA and the functional assessment of HSCs. CD34⁻KSL HSCs were sorted at 50 cells per well and were transduced with either the scramble control KD or the WAVE2 KD vector. Transduction efficiencies, assessed by GFP expression at day 4 after viral infection (day 5 after HSC preparation), were near

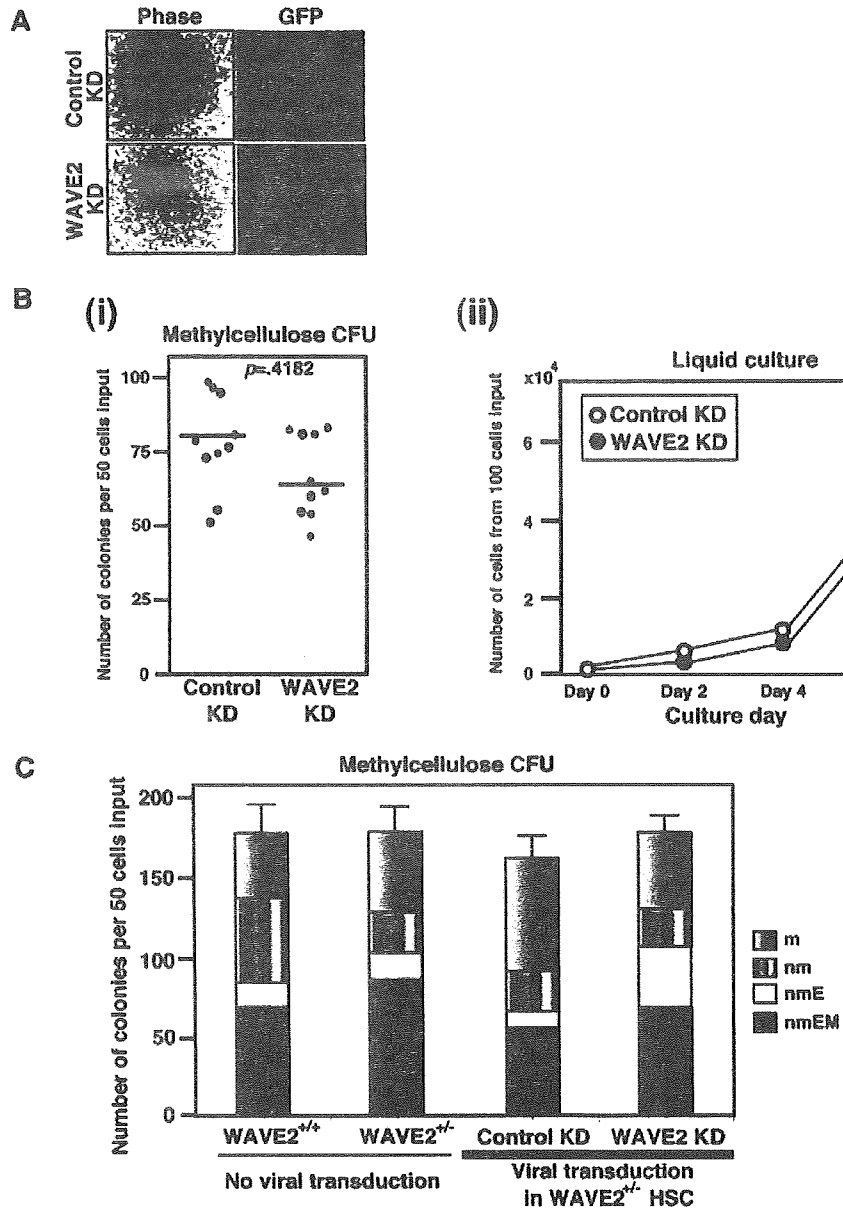

Figure 3. The KD of WAVE2 does not impair HSC colony formation in methylcellulose or HSC proliferation in liquid culture. Transduced HSCs were subjected to methylcellulose colony assays or liquid culture without stromal cells in the presence of interleukin-3, stem cell factor, erythropoietin, and thrombopoietin. **(A):** A bright-field photomicrograph (phase) and the corresponding fluorescence microscopic image (GFP) of a representative day 14 colony derived from HSCs transduced with either control short hairpin RNA (shRNA) virus (top, control KD) or WAVE2 shRNA virus (bottom, WAVE2 KD). **(B-i):** Graphic representation of the number of day 14 colonies formed by cells transduced with either control KD or WAVE2 KD virus. **(B-ii):** Graph of cell numbers per well of 96-well plates at days 2, 4, and 6 of culture when 100 GFP^+ HSCs were directly sorted into each well. Results are means ± SD ($n = 4$). A representative result of two independent experiments is shown. **(C):** Colony formation by cells derived from $WAVE2^{+/+}$ or $WAVE2^{+/-}$ $CD34^-KSL$ cells without infection and by cells derived from $CD34^-KSL$ cells from $WAVE2^{+/-}$ mice after transduction with control or WAVE2 shRNA virus. Colonies at day 14 were enumerated and classified into m, nm, nmE, and nmEM colonies. Results are means ± SD from three independent assays. Abbreviations: CFU, colony-forming unit; GFP, green fluorescent protein; HSC, hematopoietic stem cell; KD, knockdown; m, macrophage; N.S., not significant; nm, neutrophil and macrophage; nmE, neutrophil, macrophage, and erythrocyte; nmEM, neutrophil, macrophage, erythrocyte, and megakaryocyte; WAVE, Wiskott-Aldrich syndrome protein family verprolin-homologous protein.

100% in most experiments (Fig. 2B). Efficient reduction of WAVE2 expression was verified by both RT-PCR analysis and immunostaining (Fig. 2C, 2D). HSCs rendered defective in WAVE2 expression remained viable, which was confirmed by annexin V staining-based assessment of cellular apoptosis (supporting information Fig. 1). These results indicated that lentivirus-mediated KD in HSCs efficiently reduced WAVE2 expression without inducing significant levels of cell death.

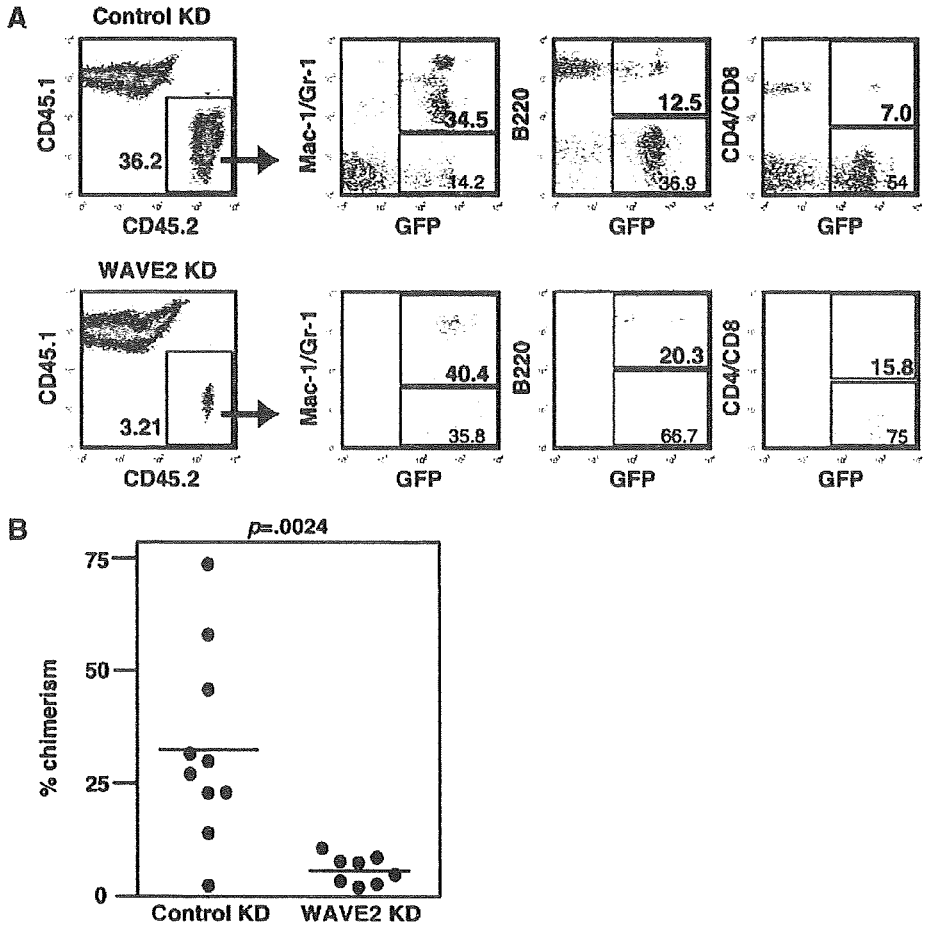

Figure 4. The KD of WAVE2 in hematopoietic stem cells (HSCs) leads to defective long-term repopulation. Transduced HSCs were subjected to competitive repopulation assays. Peripheral blood of recipient mice was examined by flow cytometry 16 weeks after transplantation. **(A):** Representative data for control KD HSCs and WAVE2 KD cohorts are shown. Both populations were transduced using either control short hairpin RNA (shRNA) (control KD) or WAVE2 shRNA (WAVE2 KD) virus. All donor cells are identified by CD45.2 expression. Transduced cells are identified by GFP expression. HSCs in both control and WAVE KD cohorts differentiated into myeloid cells (Mac-1/Gr-1$^+$ cells), B lymphocytes (B220$^+$ cells), and T lymphocytes (CD4/CD8$^+$ cells). **(B):** Scatter plots represent % chimerism 16 weeks after transplantation, calculated by (% CD45.2$^+$ cells) × 100/(% CD45.1$^+$ cells + % CD45.2$^+$ cells). WAVE2 KD HSCs exhibit low level but substantial multilineage reconstitution. Abbreviations: GFP, green fluorescent protein; KD, knockdown; WAVE, Wiskott-Aldrich syndrome protein family verprolin-homologous protein.

Functional Analyses of HSCs Rendered Defective in WAVE2 Expression

To test if lack of WAVE2 affected in vitro cell growth in HSCs, we performed methylcellulose colony assays on CD34$^-$KSL HSCs transduced with either control vector or WAVE2 KD vector. Rac1$^{-/-}$ HSPCs reportedly responded to SCF with reduced in vitro cell growth, [16] but showed a normal proliferative response to combinations of multiple cytokines [15]. The CD34$^-$KSL cell fraction used in this study represents a highly purified HSC population in which SCF alone does not support sufficient cell growth [25]. We therefore used multiple cytokines to study the proliferative responses of these cells [22, 25]. As shown in Figure 3A, CD34$^-$KSL HSCs transduced with either control virus (top) or WAVE2 shRNA virus (bottom) yielded substantial numbers of myeloid colonies (>1 mm diameter), most of which showed GFP fluorescence (>85% transduction efficiency). Interestingly, WAVE2 KD colonies appeared loose, whereas control colonies appeared compact (Fig. 3A). WAVE2 KD did not influence the frequency of colony-forming cells (Fig. 3B-i); gross proliferation in liquid culture also was not affected by WAVE2 KD (Fig. 3B-ii). In addition, WAVE2 KD HSCs exhibited no significant defect in the capability of multilineage differentiation (Fig. 3C). The observation that reduction of WAVE2 did not lead to a gross loss of HSC proliferation ability in response to multiple cytokines is consistent with data previously obtained from analysis of Rac1$^{-/-}$ HSPCs [15]. To test if WAVE2 KD affected in vivo reconstitution abilities in HSCs, we next performed competitive repopulation assays on CD34$^-$KSL HSCs transduced with either control virus or WAVE2 shRNA virus. Single-well HSCs were collected and transplanted into irradiated CD45.1 recipient mice (well:mouse, 1:1) along with 2 × 10^5 CD45.1 BM cells as competitor cells [22, 26]. Figure 4A shows a representative result of analysis of peripheral blood obtained from recipient mice 16 weeks after transplantation. Control CD45.2$^+$ HSCs showed a substantial contribution to hematopoiesis (36.2% chimerism), whereas CD45.2$^+$ HSCs in which WAVE2 expression was reduced exhibited a low level of reconstitution (3.2% of chimerism). Multicolor analyses revealed that all myeloid, B-lymphoid, and

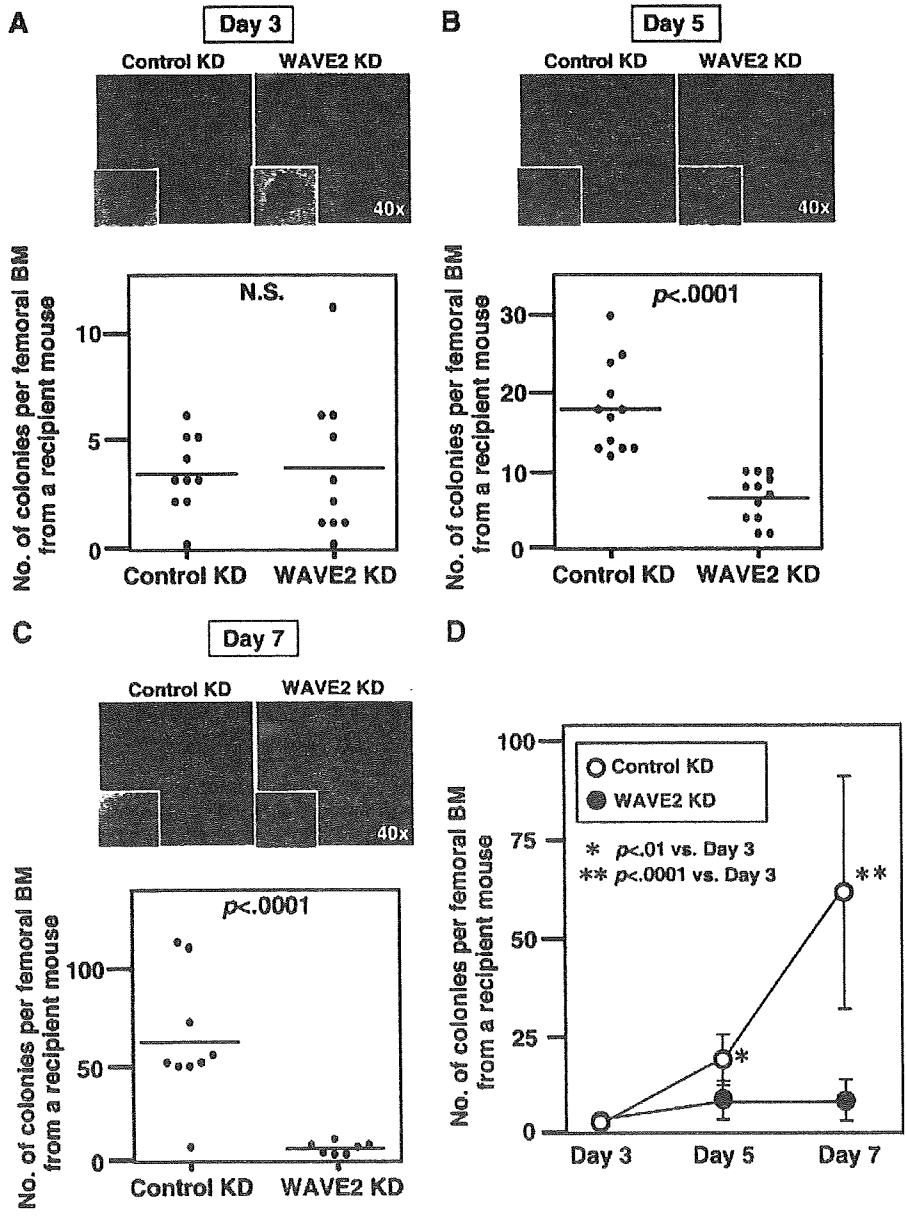

Figure 5. The KD of WAVE2 impairs early marrow repopulating activity in hematopoietic stem cells (HSCs). Whole BM cells were obtained from the femora of each lethally irradiated recipient mouse at day 3 (**A**), day 5 (**B**), or day 7 (**C**) after transplantation of HSCs transduced with either control (n = 9–12) or WAVE2 KD (n = 7–12) vector. Donor-origin colony-forming cells in femoral BM were enumerated. A fluorescence microscopic image and the corresponding bright-field picture of a representative colony are shown above each graph. (**D**): Comprehensive graphic representation of time-dependent change. Data are shown as means ± SD. Experiments were done three times independently. Pooled results are shown. Abbreviations: BM, bone marrow; KD, knockdown; N.S., not significant; WAVE, Wiskott-Aldrich syndrome protein family verprolin-homologous protein.

T-lymphoid lineages were reconstituted by GFP^+ cells (Fig. 4A). The comprehensive results obtained from two independent experiments showed that long-term repopulation levels using WAVE2 KD HSCs were significantly lower than those using control HSCs (Fig. 4B). Of note is that low but significant levels of long-term multilineage reconstitution were still detectable after transplantation with WAVE2 KD HSCs. These results indicated that either the number of long-term repopulating cells or the long-term repopulating activity was diminished in HSCs in which WAVE2 expression was reduced.

Early Repopulation by WAVE2 KD HSCs

To learn why WAVE2 KD HSCs reconstitute poorly long term, we sought to assess early in vivo kinetics of HSC repopulation within BM after transplantation. As we used a limited number of highly purified HSCs as test donor cells, it was impractical to estimate the number of donor cells homed to the BM cavity by flow cytometry or microscopy. We therefore examined how colony-forming cells of donor HSC origin sequentially appeared in recipient BM.

As shown in Figure 5A, by day 3 after transplantation with transduced cells, individual recipient mouse BM cells formed few colonies in either control or WAVE2 KD cohorts. The frequencies of CFUs rapidly increased thereafter in control HSC-transplanted BM, reaching as many as ~ 100 cells per animal by day 7 in some cases (Fig. 5B–5D). In contrast, CFUs did not significantly increase in WAVE2 KD HSC-infused BM from day 3 to day 7 (Fig. 5B–5D). As all colonies expressed GFP, they must have been derived from successfully transduced HSCs. Noteworthy is that the difference in CFU repopulation kinetics between control and WAVE2 KD cohorts is highly significant (Fig. 5D). These results

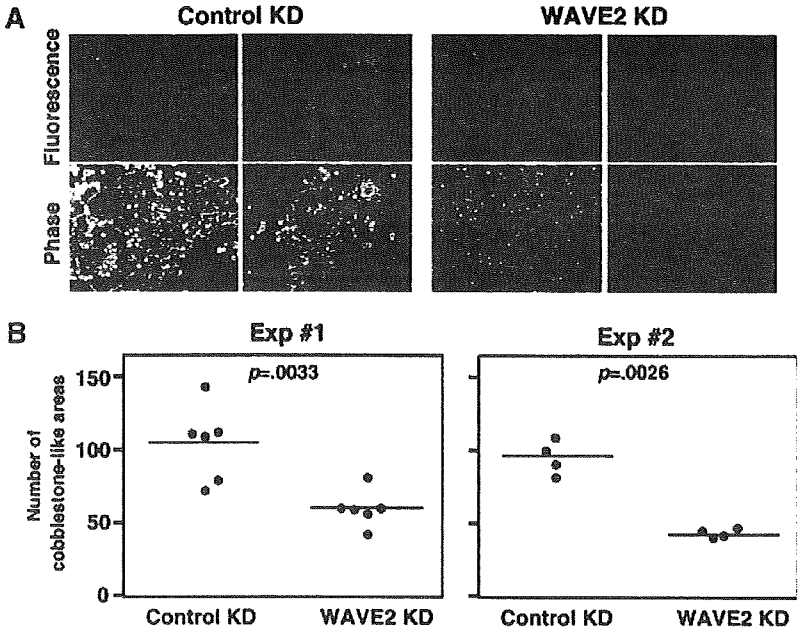

Figure 6. The KD of WAVE2 reduces the frequency of cobblestone-like area-forming cells (CAFCs). **(A):** Shown are the representative images at day 10 of cobblestone-like areas formed on C3H10T1/2 cells by either control KD or WAVE2 KD hematopoietic stem cells (HSCs). Fluorescence and phase contrast pictures are shown. **(B):** Graphic representation of the number of cobblestone-like areas. One black dot represents the number of cobblestone-like areas in a single well (6-well plates). WAVE2 KD HSCs gave rise to significantly reduced number of CAFCs. Abbreviations: KD, knockdown; WAVE, Wiskott-Aldrich syndrome protein family verprolin-homologous protein.

suggest that WAVE2 is required not for HSC homing to BM but for a repopulation process by HSCs in the BM environment.

Intact cell growth in vitro but poor repopulation in the BM environment by WAVE2 KD HSCs led us to hypothesize that WAVE2-deficiency could impair HSC functions only when HSCs were in close contact with a microenvironment that included BM stromal cells. To test this hypothesis, we conducted CAFC assays; these can assess migration activity and proliferative ability in HSCs that are in conjunction with a stromal cell layer. When sorted onto an irradiated stromal cell layer, WAVE2 KD HSCs formed cobblestone-like areas that were indistinguishable from those formed by control KD counterparts (Fig. 6A). However, the number of cobblestone-like areas formed per sorted GFP^+ HSCs was significantly lower in a WAVE2 KD cohort than in a control KD cohort (Fig. 6B), suggesting important roles of WAVE2 in HSCs for processes of colonization in the presence of stromal cells.

Discussion

Both in vitro colony-forming assays and in vivo long-term repopulation assays showed that WAVE2 KD does not affect multilineage differentiation potential in HSCs. Instead, long-term repopulation levels shown by WAVE2 KD HSCs were significantly lower than those for control HSCs (Fig. 4). We are reluctant to interpret this as an impairment of long-term repopulating or self-renewal capacity in WAVE2 KD HSCs because we still detected apparent multilineage repopulation by transduced GFP^+ cells (implying successful WAVE2 KD in most cases) 16 weeks after transplantation. We proposed instead, as likely explaining poor repopulation from WAVE2 KD HSCs, our finding that early BM repopulating activity was significantly decreased for WAVE2 KD HSCs compared with control KD HSCs (Fig. 5). On day 3 after transplantation, BM repopulation levels, as assessed by number of CFUs derived from BM, were similar for WAVE2 KD and control cohorts, indicating that WAVE2 reduction does not impair HSC homing to BM. Of particular note was that control KD HSCs rapidly repopulated the marrow by day 7 as evidenced by an increase in the number of detectable CFUs, whereas WAVE2 KD HSCs failed to expand (Fig. 5). Considering the intact cell growth in vitro in methylcellulose and liquid culture proliferation assays (Fig. 3B) and the absence of apparent cell death in WAVE2 KD HSCs (supporting information Fig. 1), it seems reasonable to conclude that any deleterious influence of WAVE2 KD on HSCs depends on the presence of the niche environment. This is supported by our observation of significantly fewer CAFCs cultured on stromal cell layers when assaying WAVE2 KD HSCs than when assaying controls (Fig. 6). Furthermore, we found impaired actin polymerization in WAVE2 KD HSCs in the presence of stimulation by fibronectin but not by poly-L-lysine (supporting information Fig. 2). This suggested that integrin ligation in the niche environment may induce or enhance the negative effects of WAVE2 deficiency on HSCs, which in turn lead to poor BM repopulation post-transplantation (Figs. 4, 7). The results of RT-PCR analysis of cell-cycle regulators may be of significant importance, because they showed that WAVE2 KD exerts some influence on the expression levels of cyclin *D1*, *p21 Cip1*, and *p27 Kip1* (supporting information Fig. 3). Because WAVE2 KD HSCs can proliferate normally in methylcellulose and liquid media (Fig. 3B), cell-cycle arrest or severe retardation is not likely. Perhaps WAVE2 KD has the potential to predispose HSCs to cell-cycle retardation, which manifests only in the BM microenvironment. Further experiments are required to prove this hypothesis formally.

This study did not address whether WAVE2 specifically acts in HSCs as a downstream effector of Rac1 but not Rac2. However, homing and repopulation properties of WAVE2 KD HSCs remarkably resembled those of Rac-$1^{-/-}$ HSPCs [14, 15]: for example, transplanted HSCs contribute poorly to long-term repopulation in both cohorts [15] (Fig. 4), and early BM repopulation is impaired in both [15] (Fig. 5). Of note is that Cancelas et al. utilized an assay system different from ours, to assess homing and lodging functions of HSPCs. By injecting a large number of wild-type c-Kit^+Lin^- BM cells labeled with carboxyfluorescein diacetate succimidyl ester

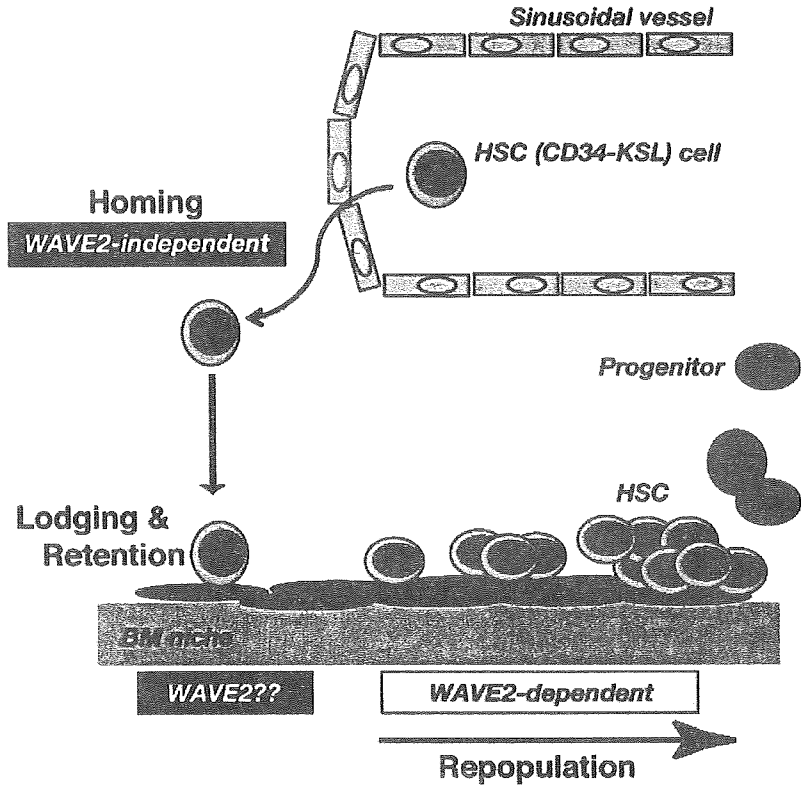

Figure 7. The putative roles of WAVE2 in HSCs in marrow repopulation after transplantation. The illustration depicts a proposed model for WAVE2 function in HSCs. WAVE2 may play a major role not in homing but in early processes of repopulation within the BM microenvironment. Abbreviations: BM, bone marrow; HSC, hematopoietic stem cell; KSL, c-Kit$^+$Sca-1$^+$lineage$^-$; WAVE, Wiskott-Aldrich syndrome protein family verprolin-homologous protein.

(CFSE) into mice, they demonstrated that CFSE-positive cells were localized preferentially in the endosteal space within 16 hours [15]. In contrast, CFSE-positive cells with Rac1 deletion showed less efficient endosteal localization (lodging failure) [15]. Interestingly, when both Rac1 and Rac2 were deleted, defects in lodging were more severe [14, 15]. Although to learn if WAVE2 KD HSCs similarly fail to lodge will be of great interest, the limited number of highly purified HSCs obtainable precluded similar studies on our part. Figure 7 illustrates the possible steps where WAVE2 is thought to play a major role in the multistep process of HSC transplantation, culminating in successful long-term repopulation.

WAVE1 and WAVE2, equally expressed in megakaryocytes and platelets [27, 28], differentially control megakaryopoiesis and platelet spreading [20]. In platelets, Rac1 is essential for lamellipodium formation, leading to stable thrombus formation in vivo [29]. Our previous studies on megakaryocytes and platelets suggest that WAVE2 but not WAVE1 is a primarily responsible target downstream of Rac1 [20]. In the developmental point of view, HSCs and megakaryocytic progenitors are closely related. WAVE2 may work as a key effector downstream of Rac1 and be required for lamellipodium formation in either HSCs or megakaryocytes.

Another Rho GTPase family member, Cdc42, is preferentially required for filopodium formation, potentially through N-WASp and WASp [11]. Yang et al. reported that in HSCs from mice conditionally deficient in Cdc42 [30], BM homing, lodging, retention, and long-term repopulation were all impaired. They also showed that Cdc42 signals positively regulate HSC quiescence, suggesting that Cdc42 is essential for physical and functional interaction between HSCs and their niches [30]. Whether these phenotypes reflect the functions of Cdc42 in normal HSCs remains uncertain, because all mice deficient in Cdc42 die because of progressive myeloproliferative disease [31]. Also reported is that the inhibition of RhoA, another Rho GTPase, by a dominant negative mutation enhances engraftment and long-term repopulation by HSPCs [32]. As all these Rho family members affect HSC functions, it will be fascinating to elucidate how their downstream signaling molecules, including WAVE2, work coordinately for proper execution of HSC functions, especially in close association with the BM microenvironment.

Conclusion

This study demonstrates that WAVE2 plays a role in an early repopulation kinetics within the BM and may act downstream of Rac1. In this regard, WAVE2 represents a new target molecule for modifying HSC engraftment in transplantation medicine.

Acknowledgments

We thank Dr. A. Knisely for manuscript review and editing and Dr. S. Suetsugu (University of Tokyo) for providing shRNA sequences of the scramble control and WAVE2. This work was supported by grants from the Ministry of Education, Culture, Sport, Science and Technology of Japan (Kakenhi to K.E., H.E., and H.N.).

Disclosure of Potential Conflicts of Interest

The authors indicate no potential conflicts of interest.

REFERENCES

1 Adams GB, Scadden DT. The hematopoietic stem cell in its place. Nat Immunol 2006;7:333–337.
2 Arai F, Suda T. Regulation of hematopoietic stem cells in the osteoblastic niche. Adv Exp Med Biol 2007;602:61–67.
3 Kiel MJ, Morrison SJ. Uncertainty in the niches that maintain haematopoietic stem cells. Nat Rev Immunol 2008;8:290–301.
4 Scadden DT. The stem-cell niche as an entity of action. Nature 2006; 441:1075–1079.
5 Nagasawa T. The chemokine CXCL12 and regulation of HSC and B lymphocyte development in the bone marrow niche. Adv Exp Med Biol 2007;602:69–75.
6 Kiel MJ, Morrison SJ. Maintaining hematopoietic stem cells in the vascular niche. Immunity 2006;25:862–864.
7 Adams GB, Chabner KT, Alley IR et al. Stem cell engraftment at the endosteal niche is specified by the calcium-sensing receptor. Nature 2006;439:599–603.
8 Adams GB, Martin RP, Alley IR et al. Therapeutic targeting of a stem cell niche. Nat Biotechnol 2007;25:238–243.
9 Scadden DT. The stem cell niche in health and leukemic disease. Best Pract Res Clin Haematol 2007;20:19–27.
10 Hall A. Rho GTPases and the control of cell behaviour. Biochem Soc Trans 2005;33 (Part 5):891–895.
11 Takenawa T, Suetsugu S. The WASp-WAVE protein network: Connecting the membrane to the cytoskeleton. Nat Rev Mol Cell Biol 2007;8: 37–48.
12 Pollard TD, Borisy GG. Cellular motility driven by assembly and disassembly of actin filaments. Cell 2003;112:453–465.
13 Miki H, Suetsugu S, Takenawa T. WAVE, a novel WASp-family protein involved in actin reorganization induced by Rac. EMBO J 1998; 17:6932–6941.
14 Cancelas JA, Jansen M, Williams DA. The role of chemokine activation of Rac GTPases in hematopoietic stem cell marrow homing, retention, and peripheral mobilization. Exp Hematol 2006;34:976–985.
15 Cancelas JA, Lee AW, Prabhakar R et al. Rac GTPases differentially integrate signals regulating hematopoietic stem cell localization. Nat Med 2005;11:886–891.
16 Gu Y, Filippi MD, Cancelas JA et al. Hematopoietic cell regulation by Rac1 and Rac2 guanosine triphosphatases. Science 2003;302: 445–449.
17 Osawa M, Hanada K, Hamada H et al. Long-term lymphohematopoietic reconstitution by a single CD34-low/negative hematopoietic stem cell. Science 1996;273:242–245.
18 Qin X-F, An DS, Chen ISY et al. Inhibiting HIV-1 infection in human T cells by lentiviral-mediated delivery of small interfering RNA against CCR5. Proc Natl Acad Sci USA 2003;100:183–188.
19 Suetsugu S, Yamazaki D, Kurisu S et al. Differential roles of WAVE1 and WAVE2 in dorsal and peripheral ruffle formation for fibroblast cell migration. Dev Cell 2003;5:595–609.
20 Eto K, Nishikii H, Ogaeri T et al. The WAVE2/Abi1 complex differentially regulates megakaryocyte development and spreading: implications for platelet biogenesis and spreading machinery. Blood 2007; 110:3637–3647.
21 Osawa M, Yamaguchi T, Nakamura Y et al. Erythroid expansion mediated by the Gfi-1B zinc finger protein: Role in normal hematopoiesis. Blood 2002;100:2769–2777.
22 Ema H, Morita Y, Yamazaki S et al. Adult mouse hematopoietic stem cells: Purification and single-cell assays. Nat Protoc 2006;1:2979–2987.
23 Yamazaki S, Iwama A, Takayanagi S et al. Cytokine signals modulated via lipid rafts mimic niche signals and induce hibernation in hematopoietic stem cells. EMBO J 2006;25:3515–3523.
24 Yamazaki D, Suetsugu S, Miki H et al. WAVE2 is required for directed cell migration and cardiovascular development. Nature 2003; 424:452–456.
25 Ema H, Takano H, Sudo K et al. In vitro self-renewal division of hematopoietic stem cells. J Exp Med 2000;192:1281–1288.
26 Ema H, Sudo K, Seita J et al. Quantification of self-renewal capacity in single hematopoietic stem cells from normal and Lnk-deficient mice. Dev Cell 2005;8:907–914.
27 Kashiwagi H, Shiraga M, Kato H et al. Expression and subcellular localization of WAVE isoforms in the megakaryocyte/platelet lineage. J Thromb Haemost 2005;3:361–368.
28 Oda A, Miki H, Wada I et al. WAVE/scars in platelets. Blood 2005; 105:3141–3148.
29 McCarty OJ, Larson MK, Auger JM et al. Rac1 is essential for platelet lamellipodia formation and aggregate stability under flow. J Biol Chem 2005;280:39474–39484.
30 Yang L, Wang L, Geiger H et al. Rho GTPase Cdc42 coordinates hematopoietic stem cell quiescence and niche interaction in the bone marrow. Proc Natl Acad Sci USA 2007;104:5091–5096.
31 Yang L, Wang L, Kalfa TA et al. Cdc42 critically regulates the balance between myelopoiesis and erythropoiesis. Blood 2007;110:3853–3861.
32 Ghiaur G, Lee A, Bailey J et al. Inhibition of RhoA GTPase activity enhances hematopoietic stem and progenitor cell proliferation and engraftment. Blood 2006;108:2087–2094.

See www.StemCells.com for supporting information available online.